Article

Powder Crystallography by Proton Solid-State NMR Spectroscopy

Bndicte Elena, and Lyndon Emsley

J. Am. Chem. Soc., **2005**, 127 (25), 9140-9146• DOI: 10.1021/ja051208t • Publication Date (Web): 04 June 2005

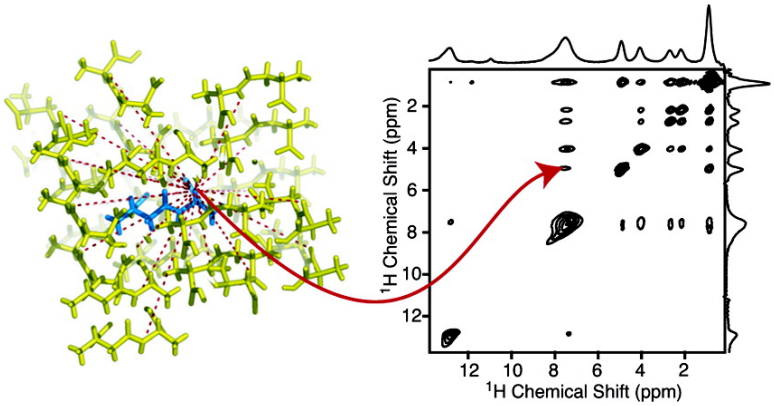

More About This Article

Additional resources and features associated with this article are available within the HTML version:

- Supporting Information
- Links to the 10 articles that cite this article, as of the time of this article download
- Access to high resolution figures
- Links to articles and content related to this article
- Copyright permission to reproduce figures and/or text from this article

View the Full Text HTML

J|A|C|S
ARTICLES
Published on Web 06/04/2005

Powder Crystallography by Proton Solid-State NMR Spectroscopy

Bénédicte Elena and Lyndon Emsley*

Contribution from the Laboratoire de Chimie (UMR 5182 CNRS/ENS), Laboratoire de Recherche Conventionné du CEA (DSV 23V/ DSM 0432), Ecole Normale Supérieure de Lyon, 69364 Lyon, France

Received February 25, 2005; E-mail: Lyndon.Emsley@ens-lyon.fr

Abstract: The investigation of $^1H-^1H$ spin-diffusion build-up curves using a rate matrix analysis approach shows that high-resolution magic angle spinning NMR of protons, applied to powdered organic compounds, provides a method to probe crystalline arrangements. The comparison between experimental ^1H data and simulation is shown to depend strongly on the parameters of the crystal structure, for example on the unit cell parameters or the orientation of the molecule in the unit cell, and those parameters are experimentally determined for a model organic compound.

1. Introduction

The development of experimental methods to study the structure of powdered solids is an area of great current interest, notably due to significant recent progress in the application of X-ray and neutron diffraction methods,[1] and to spectacular advances in solid-state nuclear magnetic resonance (NMR) methods for powdered solids.[2] This latter method has recently led to the first determination of the three-dimensional structure of a powdered microcrystalline protein,[3] and to structural models of amyloid fibrils.[4] Curiously, in some ways macromolecules are easier to handle by NMR than small molecules. For example, macromolecules can often be treated without considering the crystalline environment, and sophisticated isotopic labeling schemes are available to facilitate spectral assignment and geometry measurements. Detailed structural studies of small molecules, *especially at natural isotopic abundance*, remain challenging. Notably, NMR methods have not so far provided access to crystallographic parameters, such as the unit cell dimensions.

Solution-state NMR spectroscopy of protons is recognized as a powerful probe of molecular conformation for a large range of organic molecules. It provides the method of choice for de novo three-dimensional structure determination of biological macromolecules[5] and for conformational analysis in small molecules.[6] In contrast, in the solid state, the presence of strong dipolar couplings between protons considerably broadens the spectral resonances, even under magic angle spinning (MAS). The study of proton−proton contacts in the solid state is nonetheless particularly valuable, where possible, and such proton−proton NMR constraints are increasingly exploited for characterization of macromolecular systems,[7] mostly microcrystalline proteins, using isotopic dilution and indirect detection schemes. Spiess and co-workers have shown that double-quantum (DQ) proton NMR spectra, obtained under fast MAS, can have very important applications in nonbiological systems.[8]

The use of combined rotation and multiple pulse techniques (CRAMPS)[9] and the considerable recent advances in the field of homonuclear dipolar decoupling make the direct acquisition of highly resolved proton spectra possible.[10,11] Notably, the study of high-resolution $^1H-^1H$ transfers can be of major interest for the characterization of molecules at natural abundance, as illustrated for example by recent applications of high-resolution $^1H-^1H$ DQ MAS experiments.[12,13]

In this article we will outline a procedure that shows that the unit cell parameters can in principle be determined from proton NMR of compounds at natural isotopic abundance. We propose a simple framework for a quantitative analysis of directly

(1) Harris, K. D. M.; Cheung, E. Y. *Chem. Soc. Rev.* **2004**, *33*, 526−538.
(2) Laws, D. D.; Bitter, H. M. L.; Jerschow, A. *Angew. Chem., Int. Ed.* **2002**, *41*, 3096−3129.
(3) Castellani, F.; van Rossum, B.; Diehl, A.; Schubert, M.; Rehbein, K.; Oschkinat, H. *Nature* **2002**, *420*, 98−102.
(4) Petkova, A. T.; Ishii, Y.; Balbach, J. J.; Antzutkin, O. N.; Leapman, R. D.; Delaglio, F.; Tycko, R. *Proc. Natl. Acad. Sci. U.S.A.* **2002**, *99*, 16742−16747; Tycko, R. *Curr. Opin. Struct. Biol.* **2004**, *14*, 96−103.
(5) Wuthrich, K. *Acta Crystallogr., Sect. D* **1995**, *51*, 249−270; Cavanagh, J.; Fairbrother, W. J.; Palmer, A. G., III; Skelton, N. J. *Protein NMR Spectroscopy, Principles and Practice*; Academic Press: San Diego, 1996.
(6) Neuhaus, D.; Williamson, M. P. *The Nuclear Overhauser Effect in Structural and Conformational Analysis*; Wiley-VCH: New York, 2000.
(7) de Boer, I.; Bosman, L.; Raap, J.; Oschkinat, H.; de Groot, H. J. M. *J. Magn. Reson.* **2002**, *157*, 286−291; Reif, B.; van Rossum, B. J.; Castellani, F.; Rehbein, K.; Diehl, A.; Oschkinat, H. *J. Am. Chem. Soc.* **2003**, *125*, 1488−1489; Lange, A.; Seidel, K.; Verdier, L.; Luca, S.; Baldus, M. *J. Am. Chem. Soc.* **2003**, *125*, 12640−12648; Gehman, J. D.; Paulson, E. K.; Zilm, K. W. *J. Biomol. NMR* **2003**, *27*, 235−259; Zheng, L.; Fishbein, K. W.; Griffin, R. G.; Herzfeld, J. *J. Am. Chem. Soc.* **1993**, *115*, 6254−6261.
(8) Geen, H.; Titman, J. J.; Gottwald, J.; Spiess, H. W. *Chem. Phys. Lett.* **1994**, *227*, 79−86; Brown, S. P.; Spiess, H. W. *Chem. Rev.* **2001**, *101*, 4125−4155.
(9) Gerstein, B. C.; Pembleton, R. G.; Wilson, R. C.; Ryan, L. M. *J. Chem. Phys.* **1977**, *66*, 361−362; Gerstein, B. C. CRAMPS. In *Encyclopedia of NMR*; Grant, D. M., Harris, R. K., Eds.; Wiley: Chichester, 1996; pp 1501−1509.
(10) Vinogradov, E.; Madhu, P. K.; Vega, S. *Chem. Phys. Lett.* **2002**, *354*, 193−202.
(11) Lesage, A.; Sakellariou, D.; Hediger, S.; Elena, B.; Charmont, P.; Steuernagel, S.; Emsley, L. *J. Magn. Reson.* **2003**, *163*, 105−113.
(12) Madhu, P. K.; Vinogradov, E.; Vega, S. *Chem. Phys. Lett.* **2004**, *394*, 423−428.
(13) Brown, S. P.; Lesage, A.; Elena, B.; Emsley, L. *J. Am. Chem. Soc.* **2004**, *126*, 13230−13231.

10.1021/ja051208t CCC: $30.25

Scheme 1

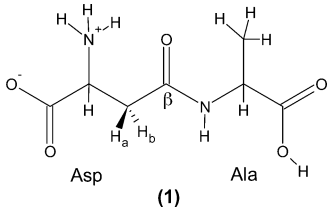

detected ^{1}H−^{1}H correlations due to spin diffusion using a phenomenological multispin kinetic rate matrix approach, summed over the structure. The approach is demonstrated through the investigation of the crystalline structure of a powdered (microcrystalline) organic model compound, β-L-aspartyl-L-alanine (**1**) (Scheme 1).

2. ^{1}H−^{1}H Spin-Diffusion Experiments

The above-mentioned improvements in spectral resolution allow us to record multidimensional proton−proton correlation spectra,[14] including spin-diffusion correlation spectra of the type shown in Figure 1, where cross-peaks between the two sites occur due to a dipolar driven spin exchange process, which takes place during the mixing time, τ_{SD}. Spin diffusion in the solid state is largely the result of a coherent and reversible process[15,16] due to dipolar couplings. Internuclear distances thus determine the kinetics of spin diffusion, but the poor resolution available from proton spectra has until now considerably limited the utilization of ^{1}H−^{1}H spin-diffusion data at the molecular level.

Our main interest here is to determine if we can correlate site resolved ^{1}H spin-diffusion dynamics to the three-dimensional molecular arrangement that comprises both the structure of an observed molecule itself as well as the full surrounding crystal packing. ^{1}H−^{1}H spin diffusion has been extensively exploited in the past for characterization of natural abundance materials at a macroscopic level,[17] but very few attempts have been described for the interpretation of ^{1}H−^{1}H spin-diffusion dynamics at a molecular scale. Diffusive models for spatial spin diffusion[18] have recently been adapted by Brus et al. to the study of initial spin-diffusion exchange rates as a probe of local molecular order.[19] Baldus and co-workers have very recently reported using ^{1}H−^{1}H contacts in combination with other data to constrain the conformation of solid L-tyrosine-ethylester, but they neglected the contribution of the crystalline environment by using isotopic enrichment methods.[20]

In the following we briefly review the mechanism for proton spin diffusion and then propose a phenomenological approach to interpreting spin diffusion dynamics at the molecular level.

Modeling Spin-Diffusion Dynamics. Theoretical models for the mechanism of spin diffusion in the solid state have been proposed widely in the past. Many of the early descriptions[16,21] were primarily aimed at so-called "spatial" spin diffusion (when the proton spectrum is not resolved). In the cases we consider, the extensions of the description to so-called "spectral" spin diffusion (between resolved protons), provided either in the static case[22] or under MAS conditions[23] are most relevant. Spectral spin diffusion arises from zero-quantum transitions that can occur when two single-quantum transitions overlap, as determined quantitatively by zero-quantum line shape function $g^{ZQ}(\omega)$. According to Kubo and McDowell,[23] under MAS a

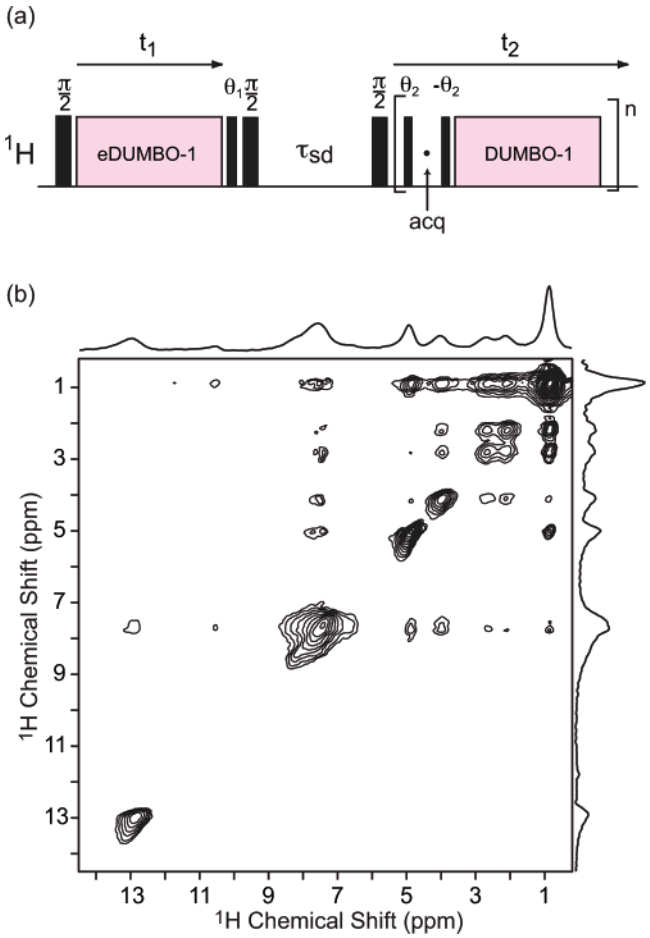

Figure 1. (a) Pulse sequence for the ^{1}H−^{1}H spin-diffusion CRAMPS detected experiment. The pulse program is available from our web site[36] or upon request. (b) 500 MHz 2D ^{1}H−^{1}H spin-diffusion spectrum of (**1**) acquired with a MAS frequency of 22 kHz, a mixing time $\tau_{sd} = 220$ μs, and a radio frequency field amplitude $\nu_1 \approx 100$ kHz. 16 transients were added with a 2.5 s repetition delay for each of the 180 complex t_1 points (96 μs t_1 increment), acquired using a States quadrature detection scheme on the second 90° pulse. The total experimental time was 2 h. For proton homonuclear dipolar decoupling during t_1 an intermediate version from the eDUMBO-1 decoupling schemes family[30] defined by Fourier coefficients $\{a_n = 0; b_1 = 0.18, b_2 = 0.21, b_3 = 0.03, b_4 = 0.12, b_5 = -0.08, b_6 = 0.125\}$ was implemented, and $\theta_1 = 1.45$ μs. During t_2, 6.3 μs windows were inserted for detection of a point every three cycles of the original DUMBO-1 decoupling scheme,[11,31] as well as short θ_2 pulses (0.5 μs) to suppress quadrature images in F_2. The total dwell time was 103.3 μs. In both dimensions, the decoupling cycles were defined with 64 phase steps of 500 ns each.

(14) Caravatti, P.; Neuenschwander, P.; Ernst, R. R. *Macromolecules* **1985**, *18*, 119−122; Sakellariou, D.; Lesage, A.; Emsley, L. *J. Am. Chem. Soc.* **2001**, *123*, 5604−5605.
(15) Zhang, S.; Meier, B. H.; Ernst, R. R. *Phys. Rev. Lett.* **1992**, *69*, 2149−2151.
(16) Meier, B. H. *Adv. Magn. Opt. Reson.* **1994**, *18*, 1−116.
(17) Demco, D. E.; Johansson, A.; Tegenfeldt, J. *Solid State Nucl. Magn. Reson.* **1995**, *4*, 13−38; Schmidt-Rohr, K.; Spiess, H. W. *Multidimensional Solid State NMR and Polymers*; Academic Press: New York, 1994.
(18) Campbell, G. C.; VanderHart, D. L. *J. Magn. Reson.* **1992**, *96*, 69−93.
(19) Brus, J.; Petrickova, H.; Dybal, J. *Solid State Nucl. Magn. Reson.* **2003**, *23*, 183−197; Brus, J.; Petrickova, H.; Dybal, J. *Monatsh. Chem.* **2002**, *133*, 1587−1612.
(20) Seidel, K.; Etzkorn, M.; Sonnenberg, L.; Griesinger, C.; Sebald, A.; Baldus, M. *J. Phys. Chem. A* **2005**, *109*, 2436−2442.
(21) Bloembergen, N. *Physica* **1949**, *15*, 386-426; Abragam, A. *Principles of Nuclear Magnetism*; Oxford University Press: London, 1961.
(22) Suter, D.; Ernst, R. R. *Phys. Rev. B* **1985**, *32*, 5608−5627; Henrichs, P. M.; Linder, M.; Hewitt, J. M. *J. Chem. Phys.* **1986**, *85*, 7077−7086; Kubo, A.; McDowell, C. A. *J. Chem. Phys.* **1988**, *89*, 63−70.
(23) Kubo, A.; Mcdowell, C. A. *J. Chem. Soc., Faraday Trans. 1* **1988**, *84*, 3713−3730.

uniform spin-diffusion time constant T_{SD} for the sample can be evaluated after integration over all crystallite orientations, for a pair of spins i and j

$$\frac{1}{T_{SD}} \propto (\omega_D^{ij})^2\Big[g^{ZQ}(\omega_R) + g^{ZQ}(-\omega_R) + \frac{1}{2}g^{ZQ}(2\omega_R) + \frac{1}{2}g^{ZQ}(-2\omega_R)\Big]$$

where ω_R is the sample rotation rate, and ω_D^{ij} stands for the magnitude of the dipolar interaction between spins i and j separated by the distance r_{ij}:

$$\omega_D^{ij} = \frac{\mu_0}{4\pi}\frac{\gamma_H{}^2\hbar}{r_{ij}{}^3}$$

The principal difficulty in analyzing spin diffusion in practice arises because g^{ZQ} is difficult to evaluate precisely. This is because we cannot simply isolate the effect of a single pair of spins, and thus any quantitative analysis of g^{ZQ} for spin-diffusion exchange must take into account a large, strongly coupled multispin system involving an ensemble of mixed distances. For example, recent studies have shown that the ZQ line shape is affected by up to hundreds of neighboring spins in the lattice.[24] Additionally, an exact description of the zero-quantum line shape function would also have to take into account the powder and MAS, which renders its estimation further complicated,[16,23] requiring time-dependent methods. The quantitative reproduction of spin-diffusion dynamics from first principles is thus a formidable challenge[16,24] and currently does not provide a practical route for structure determination.

Rate Matrix Analysis. To avoid the complexity of solving the molecular level spin-diffusion problem exactly, we propose to use a phenomenological approach to the interpretation and quantitative evaluation of spin-diffusion build-up curves observed in 2D correlation spectra. We use a model analogous to treatments developed for multisite chemical exchange,[25,26] and widely used in liquid-state NMR, using the *full* relaxation matrix protocol introduced by Macura and Ernst.[27] The analysis will relate the 2D NMR peak intensities as observed after a spin-diffusion mixing time τ_{SD}, to the full three-dimensional structure of the crystalline system through phenomenological distance-dependent rate constants.

We *assume* that in spin-diffusion experiments the evolution of the longitudinal magnetization $\mathbf{M}_z$ during the mixing time can be described by a system of coupled differential equations:

$$\frac{d\mathbf{M}_z}{dt} = -[\mathbf{K} + \mathbf{R}]\cdot(\mathbf{M}_z - \mathbf{M}_0) \quad (1)$$

where $\mathbf{M}_z$ is the instantaneous polarization along z (parallel to $\mathbf{B}_0$), and $\mathbf{M}_0$ represents the equilibrium polarization.

$\mathbf{R}$ is a matrix accounting for longitudinal relaxation during the mixing time. In this study, all relaxation processes are effective over a much longer time-scale than proton−proton spin-diffusion processes. Therefore relaxation can be neglected, and we consider in the following that $\mathbf{R} = 0$.

$\mathbf{K}$ is the kinetic matrix of rate constants that we use to describe phenomenologically the spin-diffusion exchange processes mediated by proton−proton dipolar couplings. The off-diagonal elements of $\mathbf{K}$ describe magnetization transfer between spins of type i and j and are postulated to be of the form:

$$k_{ij} = \sum_\lambda \left(\frac{\mu_0\gamma_H{}^2\hbar}{4\pi}\right)^2 \frac{A}{(r_{ij}^n)_\lambda} \quad \text{for } i \neq j \quad (2)$$

This functional form will be discussed in detail in the following section, and notably the dependence on λ which indicates exchange between i and j in different molecules in the structure. A is a phenomenological calibration constant that regulates the magnitude of the spin-diffusion exchange process. The diagonal elements of $\mathbf{K}$ are defined as the sum of all transfer rates between unlike spins:

$$k_{ii} = -\sum_{j\neq i} k_{ij} \quad (3)$$

$\mathbf{M}_z(t_1,0)$ describes the longitudinal magnetization after the second 90° pulse, before spin-diffusion exchange. Note that under our experimental conditions $\mathbf{M}_z{}^0 = \mathbf{M}_z(0,0)$ does not necessarily correspond to equilibrium polarization $\mathbf{M}_0$.[28] From eq 1, the z-magnetization after the mixing time τ_{SD} is thus given by

$$\mathbf{M}_z(t_1,\tau_{SD}) = \exp(-\mathbf{K}\cdot\tau_{SD})\mathbf{M}_z(t_1,0) \quad (4)$$

The matrix $\mathbf{P}(\tau_{SD})$, of experimentally determined peak intensities for exchange between spins i and j,

$$\mathbf{P}_{ij}(\tau_{SD}) = \exp[-\mathbf{K}\cdot\tau_{SD}]_{ij}\cdot M_{zj}{}^0 \quad (5)$$

thus provides a direct link between spin-diffusion rates and experimental intensities.[25,26,29] The kinetic matrix $\mathbf{K}$ can be diagonalized in a basis of eigenvectors $\boldsymbol{X}$. The resulting diagonal matrix of eigenvalues is noted Λ, and verifies

$$\Lambda = \boldsymbol{X}^{-1}\cdot\mathbf{K}\cdot X \quad (6)$$

Equation 4 can then be written as[26,29]

$$P_{ij}(\tau_{SD}) = [\boldsymbol{X}\exp(-\Lambda\cdot\tau_{SD})\cdot\boldsymbol{X}^{-1}]_{ij}M_{zj}{}^0 \quad (7)$$

Therefore, for a given a molecular structure, it is possible to calculate the corresponding spin-diffusion spectrum from the rate matrix $\mathbf{K}$, for each mixing time τ_{SD}, and reproduce the experimental proton−proton spin-diffusion build-up curves. (The reverse procedure is also practicable, and one could, in theory at least, given a well chosen mixing time, directly calculate $\mathbf{K}^{exp}$ from the experimental 2D correlation intensities[25]).

This rate matrix analysis thus provides a potentially very interesting alternative to handle proton spin diffusion in multispin systems. Note that this approach does not discriminate between direct dipolar contacts or relayed transfers, and the

(24) Sakellariou, D.; Hodgkinson, P.; Hediger, S.; Emsley, L. *Chem. Phys. Lett.* **1999**, *308*, 381−389; Hodgkinson, P.; Sakellariou, D.; Emsley, L. *Chem. Phys. Lett.* **2000**, *326*, 515−522.
(25) Abel, E. W.; Coston, T. P. J.; Orrell, K. G.; Sik, V.; Stephenson, D. *J. Magn. Reson.* **1986**, *70*, 34−53.
(26) Perrin, C. L.; Dwyer, T. J. *Chem. Rev.* **1990**, *90*, 935−967.
(27) Macura, S.; Ernst, R. R. *Mol. Phys.* **1980**, *41*, 95−117.
(28) Kock, M.; Griesinger, C. *Angew. Chem., Int. Ed. Engl.* **1994**, *33*, 332−334.
(29) Ernst, R. R.; Bodenhausen, G.; Wokaun, A. *Principles of Nuclear Magnetic Resonance in One and Two Dimensions*; Clarendon Press: Oxford, 1987.

model is fully valid in both situations. In the following we have chosen to simulate the experimental ^{1}H spin-diffusion build-up curves while relaxing the condition of an inverse sixth-order dependence on the internuclear distance r_{ij}, as suggested by eq 2. This leaves two variables for fitting the exchange curves, A and n, which respectively quantify the global magnitude of spin-diffusion transfers, and the functional dependence on internuclear distances.

In the following we evaluate this approach for solids, we discuss the nature of **K** and the validity of the assumptions made regarding the model.

3. Experimental Section

NMR Experiments. β-L-Aspartyl-L-alanine (**1**) was purchased from Bachem (Bübendorf, Switzerland) and used without further recrystallization. This (nonstandard) dipeptide was chosen as a typical model for small organic molecules (and should not be considered a prototype for larger macromolecular systems). All NMR experiments were conducted at room temperature on a Bruker Avance 500 (^{1}H proton frequency 500 MHz) wide-bore spectrometer, equipped with a prototype Bruker ^{1}H single channel 2.5 mm MAS probe. The general pulse scheme used for ^{1}H−^{1}H spin-diffusion experiments is depicted in Figure 1. Proton transverse magnetization is prepared by the initial 90° pulse, and ^{1}H homonuclear dipolar decoupling is achieved during t_1 using eDUMBO-1 decoupling scheme.[30] During t_1, precession occurs in a plane perpendicular to the proton decoupling effective field, and the magnetization is then brought back into the (xy) plane by a short θ_1 pulse. The following 90° pulse rotates proton magnetization toward the z-axis in preparation for the mixing period τ_{SD}. The final 90° pulse rotates the longitudinal magnetization after spin diffusion into the (xy) plane for direct proton detection using a windowed version of the original DUMBO-1 homonuclear decoupling sequence.[11,31] The short θ_2 pre-pulses were added for complete removal of quadrature image artifacts. For recording of the full proton spin-diffusion build-up curves, 14 spectra were collected with spin-diffusion mixing time τ_{SD} distributed from 2 μs to 1 ms. A proton resolution of around 0.25 ppm (after correction for the decoupling scaling factor) was achieved in both dimensions. Three different collections of 2D spectra were acquired for MAS frequencies respectively set to 6.25, 12.5, and 22 kHz.

Crystal Simulations. A full characterization of (**1**) is available from X-ray diffraction,[32] and ^{1}H coordinates were extracted directly from the deposited structure in the Cambridge Structural Database and used without re-optimization. The crystal network is orthorhombic, with four molecules contained in the unit cell according to space group $P2_12_12_1$ (as shown in Figure 2). Unit cell parameters are: a = 4.845 Å, b = 9.409 Å, c = 19.170 Å. All molecules in the unit cell are related by crystallographic symmetry elements, respectively two-fold screw axis parallel to ***a***, ***b***, and ***c*** and are magnetically equivalent.

Simulations, including construction of the crystallographic network, subsequent rate matrix analysis, and fitting of the spin-diffusion build-up curves were conducted using C++ routines and optimized matrix manipulation libraries.[33]

4. Results and Discussion

Experimental ^{1}H−^{1}H spin-diffusion curves acquired with a MAS rate of 6.25 kHz for powdered (**1**) are presented in Figure 3, together with the best fit to the data obtained using the rate matrix analysis. The fit was performed using the known X-ray crystal structure for calculation of k_{ij} from internuclear distances.

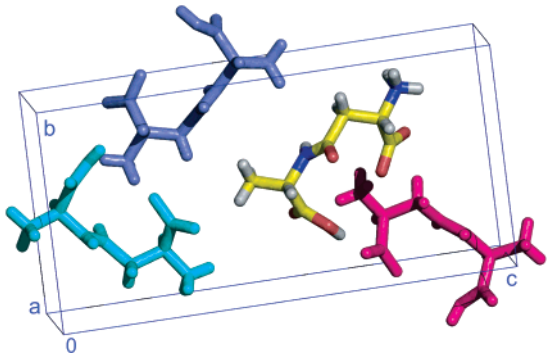

Figure 2. Crystal structure of β-L-aspartyl-L-alanine (**1**). The orthorombic unit cell (space group $P2_12_12_1$) contains four symmetry-related NMR-equivalent molecules.

(The r_{ij} were therefore not variables in the fitting procedure). The fit compares the calculated spectral intensities (**P**) for trial values of the two fit parameters, A and n, to the experimental data, with a least-squares minimization routine using the Levenburg-Marquardt algorithm. The least-squares function that characterizes the quality of the fit is:

$$\chi^2 = \sum_i \frac{(\mathrm{calc}_i - t_i)^2}{\sigma_i^2}$$

where σ_i is the estimated error on data point i. The noise level was considered constant across the spectra, and a single value of σ was used. The experimental values were obtained, for each spin-diffusion mixing delay τ_{SD}, from the volumes of the 49 resolved correlation peaks in the 2D spectra. The equilibrium values of the magnetization M_{zj}^0 were determined from integration of the diagonal peaks in the $\tau = 0$ spin-diffusion spectrum.

For calculation of the elements of the kinetic matrix, k_{ij}, according to eq 2, all contacts where taken into account for a given spin i *to all the equivalent spins* j *in surrounding molecules*, λ, (as well as in the same molecule), within a radius of 30 Å from the observed atom, i. This implies that a cross-peak between two resonances contains contributions from several different exchange processes: between the atoms within the molecule and between the atoms in different molecules in the crystalline arrangement. The sensitivity to the contacts with neighboring molecules, and the size of the crystalline system required, are described in the following.

The Crystalline Network. As reported previously for proton double-quantum correlation experiments,[13] the study of dipolar transfers in crystalline organic compounds at natural abundance must take into account equally intra and intermolecular contacts. The importance of intermolecular contacts has also been observed in the context of heteronuclear transfer.[34] As illustrated in Figure 4 for the case of (**1**), a single correlation peak corresponds to an ensemble of mixed intra- and interdistance restraints. To quantify the sensitivity of the experiments to the crystalline environment, a series of trial fits to the experimental data was carried out with different sizes of the surrounding crystalline systems. Figure 5a, shows the fit quality as a function of the cutoff distance between individual atoms considered in the fit. We see that the quality changes up to a cutoff value of about 6 Å, indicating therefore that spins up to 6 Å away from

(30) Elena, B.; De Paepe, G.; Emsley, L. *Chem. Phys. Lett.* **2004**, *398*, 532−538.
(31) Sakellariou, D.; Lesage, A.; Hodgkinson, P.; Emsley, L. *Chem. Phys. Lett.* **2000**, *319*, 253−260.
(32) Gorbitz, C. H. *Acta Chem. Scand. B* **1987**, *41*, 679−685.
(33) Hodgkinson, P. *Libcmatrix*, release 2.
(34) Brus, J.; Jegorov, A. *J. Phys. Chem. A* **2004**, *108*, 3955−3964.

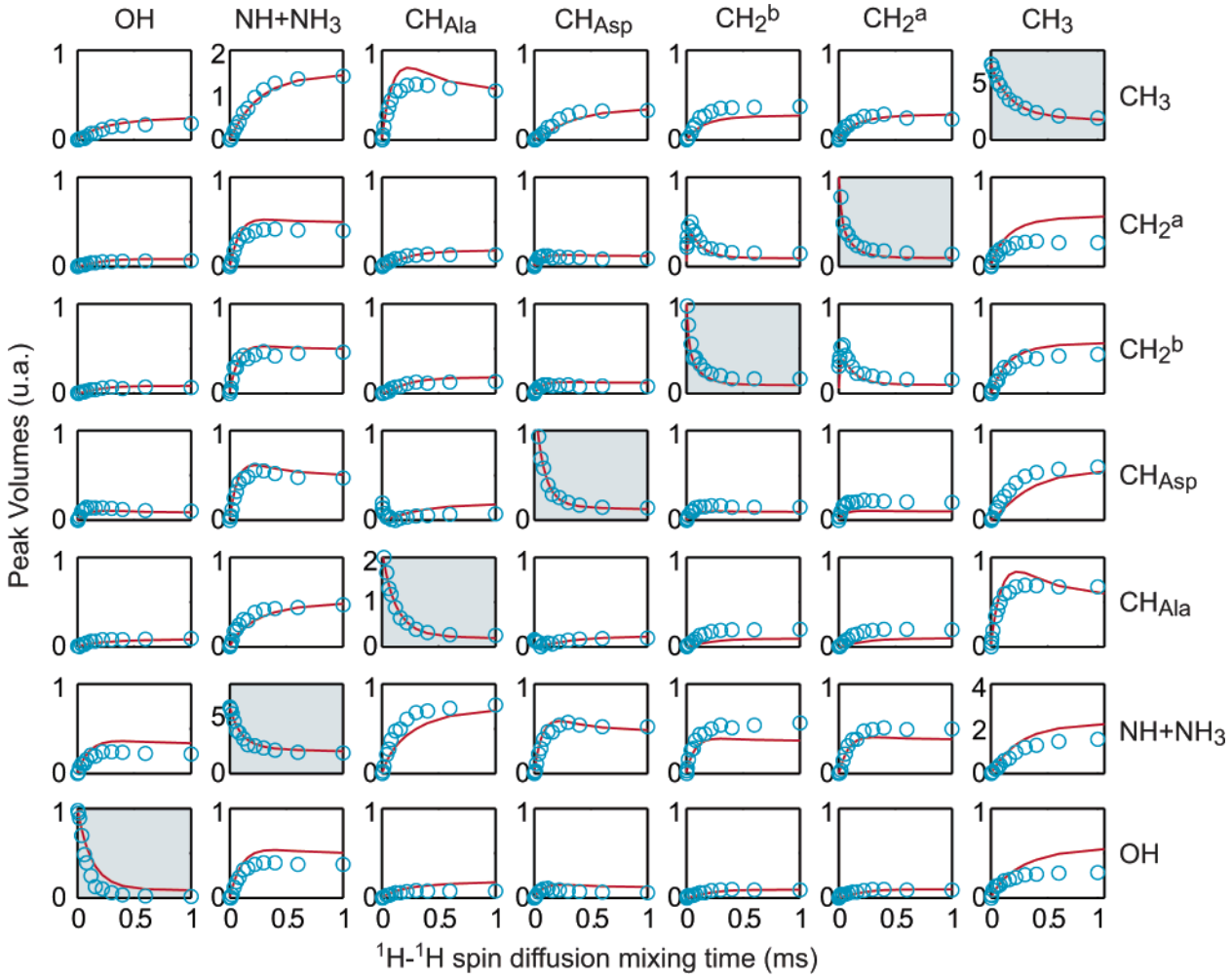

Figure 3. Representative ^{1}H−^{1}H spin-diffusion build up curves for β-L-aspartyl-L-alanine (**1**). Experimental data (○), recorded at a MAS frequency of 6.25 kHz, and best fits (red curves) from the rate matrix analysis are compared.

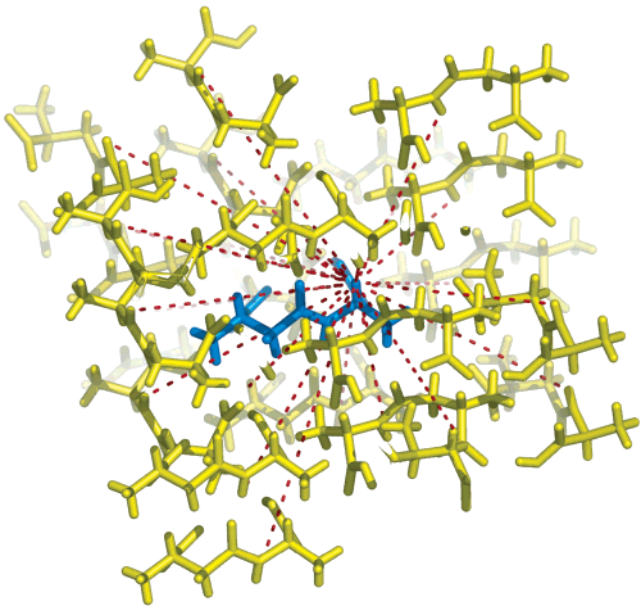

Figure 4. Representation of the NMR observed dipolar contacts corresponding to a single NH−CH^{Ala} correlation peak from 2D spin-diffusion spectra. A single molecule (blue) is depicted in its crystalline environment (yellow). Mixed intra- and intermolecular contacts (dashed) are relevant for interpretation of ^{1}H−^{1}H spin-diffusion correlation peaks.

the observed spin significantly affect the data. Adding contacts greater than 6 Å has no effect in this case. (Note that for the spin pairs taken into account, at least one of the spins is the *observed* spin, i.e., belonging to the center *observed* molecule. This prevents the simulation from including irrelevant redundant contacts that could lead to divergence of the fits when increasing the size of the system).

Even though a relatively moderate range (<6 Å) of relevant contacts could then be used for a crystal structure refinement, it is interesting to note the significance of this cutoff value in terms of the sensitivity to the molecular packing. Figure 5b shows the fit quality as a function of including intermolecular contacts with *molecules* within the radius R_{mol} (the distance between the centers of gravity of neighboring molecules). Here we see that, in our case, molecules up to 10 Å away provide distance constraints that are necessary for correct simulation of experimental data (and which consequently correspond to the presence of internuclear proximities <6 Å). These observations suggest that spin-diffusion experiments can be accurate probes of the crystalline arrangement. In particular, *the distances of observed contacts available to constrain a 3D crystal structure is comparable with the size of the unit cell.*

Determination of Unit Cell Parameters. Figure 6 shows the quality of the fit to the spin-diffusion data as a function of

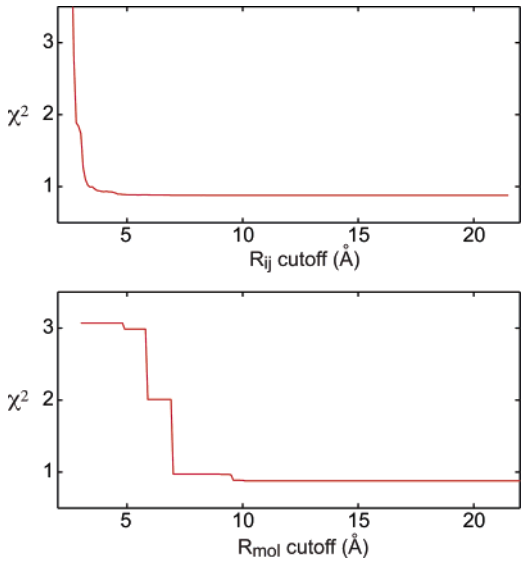

Figure 5. Quality of the fits as function of the size of the crystalline system considered for calculation. Respectively, all contacts between spins i and j (spin i belongs to the *observed* molecule I) for which $r_{ij} < R_{ij}$ cutoff (top curve), or all spin pairs (i,j) belonging to molecule I and J such as $r_{IJ} < R_{mol}$ cutoff value (bottom) are taken into account for simulation. r_{IJ} is the distance between centers of gravity of molecules I and J.

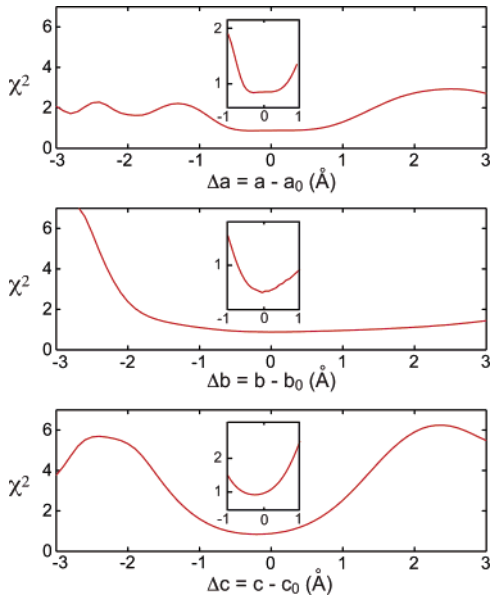

Figure 6. Quality of the fits to experimental NMR data (6.25 kHz MAS) plotted as a function of unit cell parameters deviation from their "nominal" (X-ray structure) values $a_0 = 4.845$ Å, $b_0 = 9.409$ Å, and $c_0 = 19.170$ Å. No deformation was applied to the structure of the molecule itself. All molecules within $R_{mol} = 30$ Å, build using symmetry elements of space group $P2_12_12_1$ and trial unit cell parameters $\{a, b_0, c_0\}$ (top), $\{a_0, b, c_0\}$ (middle), $\{a_0, b_0, c\}$ (bottom), were considered for simulation of the crystalline environment.

the unit cell dimensions a, b, and c. For each value of (a, b, c) the three-dimensional crystal network was built from a single molecule using the symmetry operations of the space group $P2_12_12_1$, but using unit cell parameters a, b, or c different from the *nominal* values provided by X-ray structure. The conformation of the molecule itself was fixed, identical to that of the X-ray arrangement. In the plots shown in Figure 6, one unit cell dimension is varied while the other two are kept fixed at their nominal value. These simulations clearly demonstrate a strong correlation between the quality of the fit and unit cell

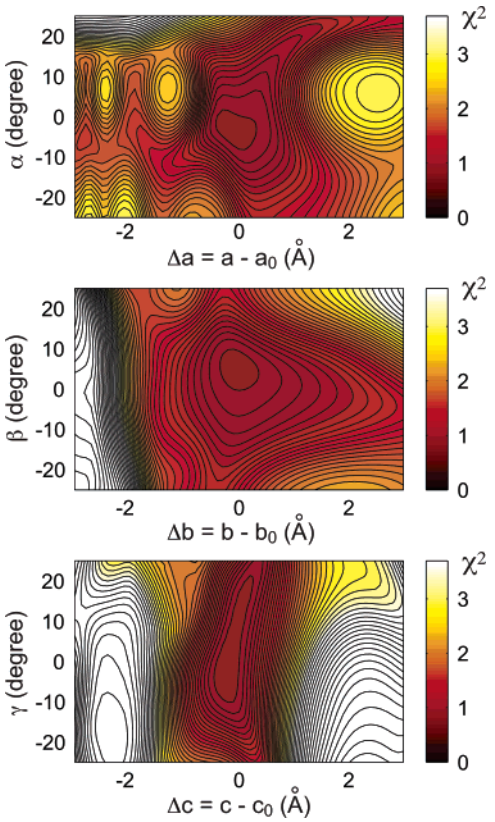

Figure 7. Quality of the fits to experimental NMR spin-diffusion data (6.25 kHz MAS) as a function of unit cell parameters and orientation of the molecules within crystal unit cell. The structure of molecules themselves is not altered. Molecular packing according to symmetry of space group $P2_12_12_1$ is distorted with respect to X-ray crystal structure with combination of unit cell parameters variations and rotation of the starting molecule within the asymmetric unit (angles α, β, and γ defined in the text). Two-dimensional slices of the six-dimensional variation space for these parameters are shown.

parameters that define the crystalline packing. In this case we could use our data to determine the unit cell dimensions, for which the best fit was obtained (where the only fit variable is A). We find $a = 4.81$, $b = 9.26$, $c = 18.96$ angstroms which are different from the X-ray values by -0.04, -0.15 and -0.21 angstroms respectively, deviations which are all within our estimated error. This type of structural variation is a particularly good test to determine if this NMR data is sensitive to the crystalline parameters, since it varies the relative proportion of the intramolecular proton−proton dipolar couplings (which are constant) compared to the intermolecular couplings which change with the cell parameters. The figure illustrates that the data is sufficient to clearly distinguish between these two contributions.

Figure 7 shows a similar study, where both a unit cell dimension, and the orientation of the molecules in the unit cell are modified around the original structure. Before building the crystalline environment with symmetry operations of space group $P2_12_12_1$, a rotation is applied to the first molecule within the asymmetric unit. The center of gravity M of this molecule is kept fixed during rotations of respective angles α, β and γ around (Mx), (My), and (Mz) axes. Once again, the NMR data appear to highly constrain the crystal structure. Small distortions (a few degrees) of the crystalline arrangement lead to significantly worse fitting of the experimental spin-diffusion 2D spectra. Consistent results were obtained from data acquired

Table 1

ω_R (kHz)	A	n	A (for $n = 6$)
6.25	2.34×10^{-9}	6.25	5.57×10^{-7}
12.5	1.77×10^{-2}	5.5	3.16×10^{-7}
22.0	1.55×10^{-9}	6.2	1.24×10^{-7}

for different MAS speeds (6.25, 12.5 and 22 kHz). Again, the reverse procedure is also feasible, and one can in principle leave these parameters as additional variables of the fit.

The phenomenological approach described above relies on initial the assumption that an average constant A can be defined to quantify multisite proton spin-diffusion exchange (eq 2). The parameter n, that gives the order for spatial dependence ($1/r^n$), is also considered as variable. In this work we have left n as a fit variable, primarily to confirm the $n \approx 6$ dependence that we expect on the basis of the best existing approximate theoretical approaches.[22,23] The n values were then determined, for each set of data at the various MAS frequencies, from an initial best-fit procedure (of parameters A and n) using the X-ray crystal structure. The parameters found in those fits are indicated in Table 1, and n was kept fixed at those values for the analysis of the sensitivity to the crystalline environment described in Figures 6 and 7. As expected, the experimentally determined n values are close to 6. The fact that the best-fit value is not always exactly 6 probably reflects minor deviations from model behavior, although the difference in the fit quality is very small. We are currently studying the significance of these effects.

As expected, MAS slows down spin-diffusion processes, and the parameter A decreases for increasing spinning frequencies ω_R (compared for a given n).

The above results clearly show that by using this simple framework, therefore, it is possible to reproduce NMR spin-diffusion data and probe crystalline arrangements, even though this model can surely be improved in the future. For example, a more accurate description including the effects of dynamics, and notably the rotation of methyl and NH_3 groups could be included.

Finally, it should be noted that variation of the structural parameters not only leads to worse fits but often will also lead to physically unreasonable structures. Combination of our data with modeling using an elementary force field would obviously further improve the results or stability of the fitting procedure. This approach, including for example the determination of the molecular conformation as well as the crystallographic parameters, requires a more sophisticated software platform than the home-written routines used here. It is currently under way in our laboratory. The spin-diffusion data can also be combined with other available NMR information, for example, carbon-13 chemical shifts. Great progress has recently been made in correlating experimental chemical shifts to structure using calculations.[35] Finally, a global approach could combine all the NMR data with data from other sources such as X-ray powder diffraction.[1]

4. Conclusion

We have shown that directly detected $^1H-^1H$ spin-diffusion CRAMPS experiments can be used for the quantitative determination of the crystallographic parameters of an ordinary powdered microcrystalline organic compound at natural isotopic abundance. The link between experimental ^1H spin-diffusion curves and the X-ray crystal structure was established through a phenomenological rate matrix analysis approach. The remarkable agreement between the data and the model appear to validate the assumptions about spin-diffusion dynamics. Dipolar coupling networks extend over relatively large distances and thus require the molecule in its full crystal environment to obtain good agreement with experiment. The comparison between experimental data and simulations was shown to depend strongly on the parameters of the crystal structure, in particular on the unit cell parameters or on the orientation of the molecule in the unit cell.

Future developments of this model for spin diffusion could be envisaged to take into account perturbing factors, such as internal molecular motions or other potential sources of inaccuracy, which have not been considered here.

Acknowledgment. We thank Dr. Paul Hodgkinson (University of Durham, UK) for very helpful support, and for making available to us the *libcmatrix* c++ libraries. We are also very grateful to Frank Engelke and Stefan Steuernagel (Bruker Biospin Gmbh, Karlsruhe) for providing us with the prototype ^1H CRAMPS probe.

JA051208T

(35) Harris, R. K. *Solid State Sci.* **2004**, *6*, 1025−1037; Strohmeier, M.; Grant, D. M. *J. Am. Chem. Soc.* **2004**, *126*, 966−977.
(36) http://www.ens-lyon.fr/CHIMIE.